

Cite this: *Phys. Chem. Chem. Phys.*, 2011, **13**, 17405–17412

www.rsc.org/pccp

PAPER

Electrogenerated chemiluminescence of triazole-modified deoxycytidine analogues in *N,N*-dimethylformamide†

Kalen N. Swanick, David W. Dodd, Jacquelyn T. Price, Allison L. Brazeau, Nathan D. Jones, Robert H. E. Hudson and Zhifeng Ding*

Received 29th June 2011, Accepted 11th August 2011

DOI: 10.1039/c1cp22116g

Triazole-modified deoxycytidines have been prepared for incorporation into single-stranded deoxyribonucleic acid (ssDNA). Electrochemical responses and electrogenerated chemiluminescence (ECL) of these deoxycytidine (dC) analogues, **1–4**, were investigated as the monomers. Cyclic voltammetry and differential pulse voltammetry techniques were used to determine the oxidation and reduction potentials of **1–4**, along with the reversibility of their electrochemical reactions. The dC analogues, in *N,N*-dimethylformamide containing 0.1 M tetra-*n*-butylammonium perchlorate as electrolyte, exhibited weak relative ECL efficiencies following the annihilation mechanism, while these efficiencies were enhanced with the use of benzoyl peroxide following the coreactant mechanism. It was shown that these nucleosides could generate excited monomers, and excimers as seen by the red-shifted ECL maxima relative to their corresponding photoluminescence peak wavelengths.

1. Introduction

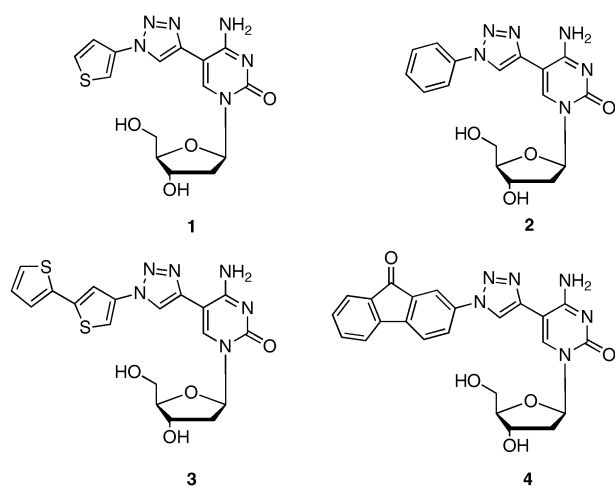
Electrogenerated chemiluminescence or electrochemiluminescence (ECL) is the process in which radicals are electrochemically generated in solution and react through electron transfer to form excited states that emit light.¹ In the 1960s, Hercules, Bard *et al.*, and Visco *et al.* reported on the first ECL studies.^{2–4} Since then, ECL has become a powerful analytical technique^{5–14} in immunoassays, food and water testing, trace metal determination, and biomolecule detection. Two main ECL systems are used: annihilation and coreactant ECL.¹ Annihilation ECL is observed when a luminophore species in solution is scanned to its first oxidation and reduction potentials at an electrode. The excited species are formed from the generation of a radical cation and a radical anion of the species in the vicinity of the electrode. The emission of light results from the excited state species. An alternative to annihilation ECL is a coreactant system, which is performed with one directional potential scanning at an electrode in a solution containing the luminophore species and an added coreactant reagent such as benzoyl peroxide, BPO.^{15,16} Radicals are generated from the luminophore, and intermediates from BPO that will decompose to produce powerful oxidizing species and react with the reduced luminophore. This generates an excited species, which upon decay emits light.

ECL applications in the detection and diagnostics of deoxyribonucleic acid (DNA) involve electrochemistry and spectroscopy, and have many distinct advantages over other spectroscopy-based detection systems¹¹ such as a lack of scattered light interference and the use of electrochemistry-based sensors¹⁷ which offer high sensitivity. In fact, a common practice to detect DNA *via* ECL is to immobilize luminophore-labelled DNA double or single strands at an electrode,^{18,19} which can be measured with the emitted light upon redox reactions of the luminophore along with a coreactant in the solution. The immobilized single strands can be employed to recognize complementary strands followed by ECL detection.^{19,20} Modified nucleosides could find potential applications as luminescent probes incorporated into single-stranded deoxyribonucleic acid (ssDNA) for sequence interrogation using ECL methods.^{20,21} Single nucleotide polymorphisms (SNPs) are single-base variations in the genetic code that occur about once every 1000 bases along the 3-billion base pair human genome.²² The ability to detect SNPs is of prime importance as mutations can be directly responsible for, or make one more susceptible to diseases such as asthma, diabetes, atherosclerosis, schizophrenia, and various cancers.²² Fluorescent modified nucleosides, when in the context of an oligomer, are potential candidates for the detection of nucleic acids with single nucleobase variations.^{23–28}

Modifications of nucleosides in nucleic acid chemistry are well established.^{29–31} However, there have been a few reports on modified deoxycytidine (dC) nucleosides,^{32–35} although the ECL behaviour of tris-2,2'-bipyridylruthenium(II) (Ru(bpy)₃²⁺) has been widely studied since the 1970s.³⁶ In the above context, Ru(bpy)₃²⁺ can be attached to a target ssDNA as an ECL label, then hybridize with its complementary strand of ssDNA immobilized on the surface of an electrode to measure the ECL

Department of Chemistry, The University of Western Ontario, 1151 Richmond Street, London, Ontario N6A 5B7, Canada. E-mail: zfding@uwo.ca; Tel: +1 519 661 2111 x86161

† Electronic supplementary information (ESI) available. CCDC reference numbers [CCDC NUMBER(S)]. For ESI and crystallographic data in CIF or other electronic format see DOI: 10.1039/c1cp22116g



Scheme 1 Molecular structures of compounds 1–4.

response of the double-stranded DNA (dsDNA). Our objective was to create a metal-free DNA sensor based on dC in combination with ECL for the detection of SNPs.

Our group previously synthesized triazole-modified deoxycytidine nucleosides, **1–4** (Scheme 1).^{37,38} These compounds are easy to prepare, and are potential candidates for use as metal-free ECL labels that can be incorporated into ssDNA for the detection of SNPs. The modified nucleosides contain four different aromatic groups, **1–4**, that have been appended to dC as desirable targets for potential uses in nucleic acid chemistry. Compound **2** has been reported previously although characterization data were lacking.³²

Here we report the electrochemical behaviour of these triazole-containing dC nucleosides, **1–4**, employing cyclic voltammetry (CV) and differential pulse voltammetry (DPV). ECL of these four compounds were also investigated *via* annihilation by scanning between the first oxidation and reduction potentials, and coreactant mechanisms by adding BPO and scanning the potential in the cathodic region. The majority of DNA-based biosensors have used uracil for studies.^{39,40} At the time of writing, there were no reports of ECL of any modified dC nucleosides in the literature.

2. Experimental

2.1 Chemicals

Commercial products and chemical reagents were used as received. 9,10-Diphenylanthracene (DPA, 97%), benzoyl peroxide (BPO, reagent grade, $\geq 98\%$) and ferrocene (Fc, 98%) were purchased from Aldrich (Mississauga, ON). The supporting electrolyte, tetra-*n*-butylammonium perchlorate (TBAP, electrochemical grade), was purchased from Fluka. All solutions were prepared using anhydrous *N,N*-dimethylformamide (DMF, 99.8%) in a Sure/Seal™ bottle, bought from Aldrich, that was immediately transferred into an N₂-filled drybox prior to use.

2.2 Synthesis of modified triazolyldeoxycytidine nucleosides

The synthesis of compounds **1–4** (Scheme 1) was published elsewhere.³⁸ In brief, these compounds were obtained by

performing a click reaction, using the Huisgen 1,3-dipolar cycloaddition reaction which is the premier example of a click reaction between alkynes and azides.^{41,42} The selective 1,4-disubstituted products of the click reaction were obtained by using a copper(I) catalyst.^{43,44} Compounds **1–4** were synthesized by reacting 5-ethynyldeoxycytidine with one of the four corresponding aryl azides in the presence of a Cu(I) catalyst, generated from CuSO₄ and sodium ascorbate, in a 1 : 1 THF–H₂O solution. The crude products of **1–4** were purified using column chromatography and characterized by ¹H and ¹³C{¹H} NMR spectroscopies and HRMS.³⁸ The purified triazole-containing compounds were then used for CV, DPV and ECL analysis.

2.3 Electrochemical preparation

CV, DPV and ECL experiments were conducted using a 2 mm diameter Pt disc inlaid in a glass sheath as the working electrode (WE), a coiled Pt wire as the counter electrode (CE), and a coiled Ag wire as the quasi reference electrode (RE). Prior to an experiment, the electrochemical cell was rinsed with acetone and deionized water, then immersed in 5% KOH in isopropanol for 4 h. The cell was rinsed with copious amounts of deionized water, immersed in 1% HCl for 4 h, and finally thoroughly rinsed with ultrapure water. The cell was dried at 120 °C for 12 h, and then cooled to room temperature.

The CE and RE were rinsed with acetone and ultrapure water, then sonicated in DMF for 15 min, in ethanol for 5 min, and finally in ultrapure water for 5 min before being thoroughly rinsed again with ultrapure water. The electrodes were then dried at 120 °C for 5 min, then left to cool to room temperature.

The WE was polished with a felt polishing pad using a 1.0 μm alumina suspension in ultrapure water (Milli-Q, Millipore) for 5 min followed by a 0.05 μm alumina suspension in ultrapure water to obtain a mirror surface and finally washed with copious amounts of ultrapure water (Buehler Ltd., Lake Bluff, IL). Then the WE electrode was electrochemically polished by cycling in 0.1 M aqueous H₂SO₄ solution for 400 segments between the potentials of 1.400 and –0.600 V at 0.5 V s^{–1} to obtain a clean and more reproducible Pt surface.⁴⁵ The oxidation and reduction of H₂SO₄ produce an ordered structure of polycrystalline Pt surfaces.⁴⁶ The electrodes were then washed repeatedly with ultrapure water, then dried with a stream of Ar gas over the Pt disc area and left to dry for 12 h at room temperature.

All solutions for electrochemical and ECL experiments were prepared in the electrochemical cell placed inside an N₂-filled drybox that possessed little oxygen and moisture. The solutions of **1–4** were in the concentration range between 2.0 × 10^{–3} and 2.7 × 10^{–3} M in anhydrous DMF (Sure/Seal™ bottle from Aldrich) containing 0.1 M TBAP as supporting electrolyte. For coreactant systems, 5.0 × 10^{–3} M BPO was added to each solution of **1–4**. The electrodes were immersed in the solution and connected by a copper wire inserted through the air-tight Teflon cap. The assembly was moved out of the drybox to perform electrochemistry and ECL experiments. After completion of each experiment, the electrochemical potential window was calibrated using Fc as the

internal standard. The redox potential of Fc/Fc^+ was taken as 0.470 V vs. NHE.⁴⁷

2.4 Electrochemical instrumentation

The CVs were conducted on a CHI 610A electrochemical analyzer (CH Instruments, Austin, TX). The experimental parameters for CVs are listed here: 0.000 V initial potential in the experimental scale, positive or negative initial scan polarity, 0.1 V s^{-1} scan rate, 4 sweep segments, 0.001 V sample interval, 2 s quiet time, $1-5 \times 10^{-5}$ A V^{-1} sensitivity. The potential range depended on the particular compound.

Four DPVs were taken for each compound on the CHI 610A, two for anodic scans (forward and reverse scans in the experimental potential scale between 0.000 V and the upper limit potential value of the compound obtained from CV experiments) and two for cathodic scans (forward and reverse scans in the experimental potential scale between 0.000 V and the low limit potential value of the compound obtained from CV experiments). The experimental parameters for DPVs are as following: 0.004 V increments, 0.05 V amplitude, 0.5 s pulse width, 0.0167 s sampling width, 0.2 s pulse period, 2 s quiet time, $1-5 \times 10^{-5}$ A V^{-1} sensitivity.⁴⁵

2.5 ECL instrumentation

The ECL cell was specifically designed to have a flat Pyrex window at the bottom for detection of generated light from the WE and was sealed with a Teflon cap with a rubber O-ring for CV, DPV, and ECL measurements. The ECL data along with CV data were obtained using the CHI 610A coupled with a photomultiplier tube (PMT, R928, Hamamatsu, Japan) held at -750 V with a high voltage power supply. The ECL collected by the PMT under the flat Pyrex window at the bottom of the cell was measured as a photocurrent, and transformed into a voltage signal, using a picoammeter/voltage source (Keithley 6487, Cleveland, OH). The potential, current signals from the electrochemical workstation, and the photocurrent signal from the picoammeter were sent simultaneously through a DAQ board (DAQ 6052E, National Instruments, Austin, TX) in a computer. The data acquisition system was controlled using a custom-made LabVIEW program (ECL_PMT610a.vi, National Instruments, Austin, TX). The photosensitivity on the picoammeter was set manually in order to avoid the saturation.

ECL pulsing experiments were conducted by using a potentiostat (Model AFCBPI, Pine Instrument Co., Grove City, PA), an EG&G PAR 175 Universal Programmer (Princeton Applied Research, Trenton, NJ), and the PMT with the picoammeter in a similar manner. The assembly was able to perform the pulsing experiments without a delay in a relative fast time pace. The data acquisition for the current, potential and ECL signals was carried out using another homemade LabVIEW program (ECL_PAR610a.vi). For coreactant systems, the applied potential was pulsed at the WE in the cathodic region (in the experimental potential scale between 0 and the low limit potential value for the compound reduction as obtained from CV experiments) with a pulse width of 0.1 s or 10 Hz.

The ECL spectra were obtained by replacing the PMT with a spectrometer (Cornerstone 260, Newport, Canada) attached to a CCD camera (Model DV420-BV, Andor Technology, Belfast, UK). The camera was cooled to -55 °C prior to use, and controlled by a computer for operation and data acquisition. The intensities *versus* wavelengths (spectra) were recorded by Andor Technology program. Similar to the pulsing experiments, the samples were pulsed at 10 Hz within each compound's potential window. The exposure time of the spectra was set to 60 s for both the annihilation and coreactant systems. Vertical lines/spikes observed in the spectra were from cosmic rays from the CCD camera.

2.6 ECL efficiency calculations

ECL quantum efficiencies (QE) were calculated relative to DPA (the reported relative ECL efficiency, Φ_{ECL} , of DPA was taken 100% or 1.0 in DMF)^{48,49} by integrating both the ECL intensity and the current value *versus* time for each compound, as described in eqn (1),^{10,50,51}

$$\Phi_x = 100 \times \left(\frac{\int_a^b \text{ECL} dt}{\int_a^b \text{Current} dt} \right)_x \bigg/ \left(\frac{\int_a^b \text{ECL} dt}{\int_a^b \text{Current} dt} \right)_{\text{st}} \quad (1)$$

where x stands for the compound (1–4) and st represents DPA.

3. Results and discussion

3.1 Electrochemistry and its correlation to electronic structures

The electrochemical behaviours of compounds 1–4 were studied in order to determine the oxidation and reduction potentials. Fig. 1 shows the CVs of 1 in DMF solution containing 0.1 M TBAP as supporting electrolyte and the blank DMF solution containing 0.1 M TBAP at a scan rate of 0.1 V s^{-1} within potential ranges between 0.000 and 2.169, and between 0.000 and -1.889 V, respectively. When the potential was scanned initially from 0.000 to 2.169 V, compound 1 underwent the first oxidation at a peak potential of 1.858 V followed by a continuous rise in current in the potential scan until 2.169 V. There was no cathodic peak when the applied potential was scanned back, indicating the irreversibility of the electrochemical oxidation reaction. The radical cations might

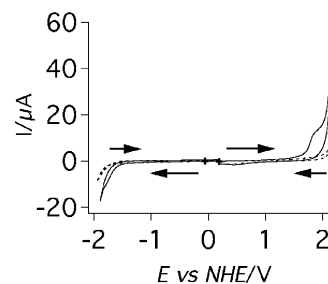


Fig. 1 Cyclic voltammograms of 1 (solid lines) in DMF containing 0.1 M TBAP as supporting electrolyte, and blank solution (dotted lines), with the initial scan from 0.000 to 2.169 V (anodic scan), and the initial scan from 0.000 to -1.889 V (cathodic scan), with a scan rate of 0.1 V s^{-1} .

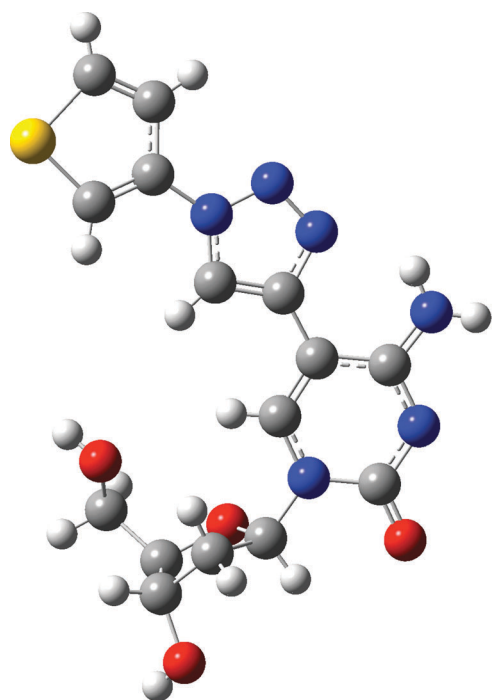


Fig. 2 Ball-and-stick representation of **1**. Except for OH and NH₂ protons, H-atoms are omitted for clarity. Please see Fig. S2, in the ESI† for labeled atoms. The final solution was submitted to the IUCR CIF checking program and had some Alert level A's or B's associated with the lack of complete data, however the general structure can be observed for **1**, similar to our previously reported solid state structure of **2**.³⁸

undergo further chemical reactions (EC mechanism). From Fig. S4 (ESI†) of our previous publication, the HOMO orbital revealed by the density function theory calculation is the linear combination of p_z atomic orbitals of S, C, N and O atoms in the thiophene, triazole and deoxycytidine rings.³⁸ The electron withdrawn from compound **1** upon oxidation was delocalized in the molecule because of the co-planar structure determined by X-ray crystallography (Fig. 2). Note that the crystal structure is our best estimation since it did not pass cif file checking (see details in the ESI†). Similarly, compound **1** demonstrated an irreversible reduction peak at −1.835 V when the applied potential was scanned from 0.000 V to the cathodic region. Based on the DFT calculation, the LUMO orbital was mostly contributed from p_z atomic orbitals of S, C and N atoms in the thiophene and triazole rings. Dimerization would probably happen on the thiophene ring. It should be noted that some small multiple oxidation and reduction peaks were observed in consecutive cycling of the applied potential, due to the electrochemical reactivity of the intermediates from the EC reaction mechanisms (see more details in the ECL section).

Typical DPVs of compound **1** conducted in a similar manner as in CVs shown in Fig. 1 are illustrated in Fig. 3, where the first irreversible oxidation and reduction peaks of **1** are well displayed. Again, isolation of the anodic and cathodic DPVs avoids any additional redox peaks as seen in Fig. 4. This agrees well with the observation from CVs because of the electrochemical reactivity of the intermediates.

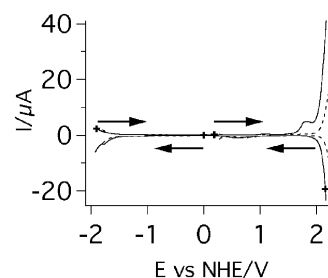


Fig. 3 Differential pulse voltammograms of **1** (solid lines) in DMF containing 0.1 M TBAP as supporting electrolyte, and blank solution (dotted lines), with the initial scan from 0.000 to 2.118 V (top, anodic scan), and the initial scan from 0.000 to −1.929 V (bottom, cathodic scan) and their reverse scans.

The formal potentials ($E^{0'}$) of **1** can be determined from DPVs by eqn (2):^{52,53}

$$E^{0'} = E_{\max} + \Delta E/2 \quad (2)$$

where E_{\max} represents the peak potential in the DPV and ΔE represents the pulse height (50 mV).

The oxidation peak at 1.826 V in the anodic scan and the reduction peak at −1.785 V in the cathodic scan were more visible (Fig. 3), than in CV (Fig. 1) since DPV suppresses the background signal and enhances sensitivity.⁴⁵

The electrochemical behaviours of compounds **2–4** were also characterized using CV and DPV, from which it can be concluded that compounds **2–4** undergo irreversible oxidation and reduction reactions, and their radical cations and anions are not stable.

All the electrochemical data have been summarized in Table 1. The electrochemical gaps, which are the potential difference between the formal potentials of the first reduction and oxidation, match well with their corresponding HOMO–LUMO energy gaps. The excited state gap taken from the PL emission wavelength from Table 2 shows similar energy values as the experimental energy values in Table 1.

From Table 1, there was a general trend of decreasing oxidation potential with increasing conjugation. The addition of a second thiophene ring in **3** decreases the oxidation potential from 1.851 V in **1**, to 1.488 V in **3**. This trend, however, was not apparent in the reduction potentials of **1–4**. Noticeably, compound **4** underwent up to 4 reduction reactions as summarized in Table 1. Nevertheless, the trend of smaller electrochemical gaps, as seen in CV and DPV, with increasing conjugation was observed from our experimental

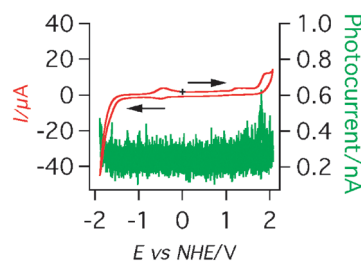


Fig. 4 Cyclic voltammogram and ECL–voltage curve of **1** scanned at 0.1 V s^{−1} with the initial potential at 0.000 to 2.069 V then scanned to −1.889 V and back to 0.000 V.

Table 1 Electrochemical (from DPV) and quantum chemistry calculation data of compounds **1–4**

	$E_{p,a}$ oxidation ^a /V	$E_{p,c}$ reduction ^a /V	$E^{0'}$ oxidation ^a /V	$E^{0'}$ reduction ^a /V	Electrochemical gap/eV	Theoretical HOMO ^c /eV	Theoretical LUMO ^c /eV	Theoretical HOMO–LUMO gap/eV
1	1.826	–1.785	1.851	–1.810	3.66	–5.90	–1.74	4.15 ^b
2	1.268	–2.081/ –2.449	1.293	–2.106/ –2.474	3.40	–5.88	–1.70	4.18 ^c
3	1.463	–1.948	1.488	–1.973	3.46	–5.90	–1.96	3.94 ^c
4	0.765/1.365	–1.310/ –1.550/ –1.806/ –2.480	0.790/1.390	–1.335/ –1.575/ –1.831/ –2.505	2.13	–5.93	–3.02	2.92 ^c

^a In V vs. NHE at 0.1 V s^{–1} scan rate. ^b Energy value obtained from previously reported data, DFT/B3LYP/6-31G* calculations.³⁸ ^c Energies obtained from DFT/B3LYP/6-31G* calculations.

Table 2 ECL data of compounds **1–4** in annihilation and coreactant systems

	Annihilation scanning QE ^a /%	Scanning QE ^a /%	Coreactant pulsing QE ^a /%	λ_{max} /nm	PL λ_{max} /nm	Shifts ^b $\lambda_{max}(\text{ECL}) - \lambda_{max}(\text{PL})/\text{nm}$
1	0.40–0.52	0.33–1.48	0.71	515	375	140
2	0.39–0.41	0.73–0.86	0.20	395/577	380	15/197
3	0.71–1.08	0.24–0.39	0.25	588	380	208
4	0.10–0.24	0.54–2.33	1.87	556	385	171

^a ECL quantum efficiencies (QE) measured in DMF relative to DPA ($\Phi_{\text{ECL}} = 100\%$ or 1.0 in DMF).^{48,49} ^b The shifts represent the difference between the ECL (in DMF) and PL (in EtOH)³⁸ emission wavelengths. Only small shifts (<5 nm) in PL emission maxima were observed when varying the solvent composition from EtOH to DMF.

data and from previous DFT quantum chemistry calculations that our group has reported.³⁸ Here, the HOMO–LUMO gap decreases in **3**, 3.94 eV, relative to **1**, 4.15 eV, having greater delocalization of the π electrons due to increased conjugation in the aromatic system, Table 1. For compounds **1** and **2**, the gaps, of 4.15 eV and 4.18 eV, were larger due to smaller conjugated systems. Synthesizing compounds with an additional thiophene ring, **3**, and extended aromatic system, **4**, the HOMO–LUMO gaps for these conjugated systems decreased to 3.94 eV for **3** and 2.92 eV for **4**. These values followed a similar trend as the experimental HOMO–LUMO gaps from the oxidation and reduction potentials of **1–4** as seen in Table 1. The gap observed in **2** from experimental data was smaller, 3.40 eV, than **1**, 3.66 eV, this may be due to the slightly out-of-plane aromatic system of **1** compared to the in-plane system of **2**. However, the HOMO–LUMO gap calculations were calculated from a solid-state representation of each compound, whereas, the redox, ECL and spectral data were obtained from solutions of these compounds. We must take into consideration the free rotation of the compounds in solution. Here, we would expect variations in the data as seen in the differences between the theoretical and experimental data.

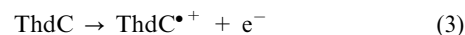
3.2 ECL via annihilation mechanisms

Fig. 4 shows the CV overlaid with the ECL–voltage curve of **1** that was run simultaneously in the potential range between its first oxidation and reduction peaks.

During these continuous scans, we observed additional bumps/peaks in the middle of the potential window. These peaks were not from the neutral compound as demonstrated in Fig. 1: when the applied potential was scanned separately for oxidation and reduction peaks, these additional peaks were not present. In addition, there was neither a cathodic peak for

oxidation and nor an anodic peak for reduction in CVs (Fig. 1). This is evidence that both radicals were not stable. Cations underwent chemical reactions to generate reduction-active species while radical anions generated redox-active species. However, we cannot determine which are the species.

At both positive and negative potential limits, weak ECL was observed. A slightly stronger emission of light was observed in the positive potential region. The radical cations appear to be more stable than the radical anions for **1**, as stronger ECL was detected in the region of positive potential, Fig. 4. The weak ECL was expected since both radical cations and anions were not stable as observed from the irreversibility of its electrochemical behaviours. The ECL given off from **1**, written as ThdC, was proposed *via* annihilation of radical cations (ThdC^{•+}) with radical anions (ThdC^{•–}) generated electrochemically, eqn (3) and (4).



An excited species, ThdC*, and a ground-state species, ThdC, of **1**, are the products of the annihilation as seen in eqn (5). The excited species then relaxes to its ground state, ThdC, as seen in eqn (6) and emits light.

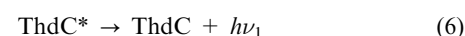
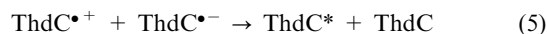


Fig. 4 also shows that ECL can only be detected after one complete cycle of the potential sweep. In practice, two cycles or four segments of the potential sweep were conducted for each compound.

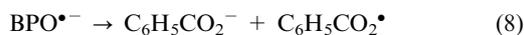
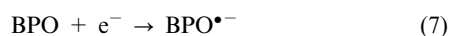
Compound **2** displayed similar ECL emission to that from compound **1**, and demonstrated stronger ECL intensity in the

anodic region than in the cathodic region. For **3**, ECL emission was observed in the region of negative potential and **4** did not show a significant increase in positive or negative potential regions. Nevertheless, weak ECL was generated through annihilation mechanisms from compounds **3–4**, because of the irreversible redox reactions, resulting in unstable radical ions. The ECL efficiencies were determined as the photons emitted per redox event relative to the standard, DPA, as expressed in eqn (1).⁵⁰ These ECL efficiencies (Table 2) were low relative to the standard, which were in a range between 0.40 to 0.52% for **1**, 0.39 to 0.41% for **2**, and 0.71 to 1.08% for **3**. Compound **4** had the smallest ECL efficiency, ranging between 0.10 to 0.24%.

3.3 ECL via coreactant mechanisms

Fig. 5 shows the CV overlaid with the simultaneous ECL–voltage curve of **1** containing BPO. The applied potential was only needed to scan in the cathodic region. In this way the short-life radical anions, ThdC^{•−}, generated can immediately react with their counterparts.^{1,54} Sometimes the radical cations can be generated directly from the coreactant.

It was discovered that ECL was enhanced when 5.0×10^{-3} M BPO was added to the solutions of **1–4**. The proposed ECL coreactant mechanism for **1** begins when a negative potential is applied to the system, initially at 0.000 V, as seen in Fig. 5 for compound **1**. Upon scanning to more negative potential, BPO is first reduced to its radical anion, BPO^{•−}, at −0.780 V, eqn (7). The radical anion, BPO^{•−}, immediately decomposes to form a strong oxidizing intermediate radical, C₆H₅CO₂[•], and C₆H₅CO₂[−], eqn (8). This intermediate radical, C₆H₅CO₂[•], reacts with **1** and generates the radical cation of **1**, ThdC^{•+}, eqn (9).



With the applied potential scanned to more negative potential, the radical anion of **1**, ThdC^{•−}, was generated at −1.835 V, eqn (4). The radical cation, ThdC^{•+}, combines with the radical anion, ThdC^{•−}, and generates an excited species, ThdC*, of **1**, as stated previously with the annihilation mechanism in eqn (5) and (6), which relaxes down to its ground state, ThdC, and light is emitted.

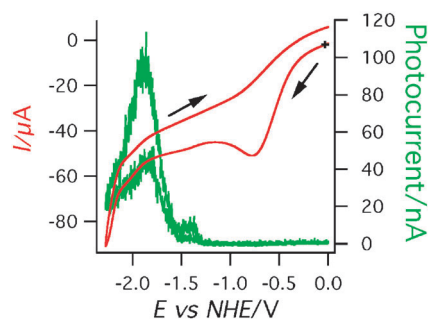


Fig. 5 Cyclic voltammogram and ECL–voltage curve of **1** with 5.0×10^{-3} M BPO scanned at 0.1 V s^{-1} , with the initial scan from 0.000 to −2.278 V and back to 0.000 V.

An increase in photocurrent as shown in Fig. 5 was observed when scanning to the negative potential. The use of BPO contributes to the enhanced ECL intensities of **1–4** relative to the intensities observed in annihilation studies.

It is important to note that there was a relatively weak ECL peak in Fig. 5 that was observed right after the BPO reduction potential, −0.780 V, but even before the reduction of compound **1**. In fact, the ThdC^{•+} generated through reactions (7)–(9) can react with BPO^{•−}, eqn (10), to produce the excited species, ThdC*:



Compounds **2–4**, in the same coreactant system, displayed higher intensities of ECL than in annihilation systems relative to DPA as seen in Table 2. ECL was observed in all compounds after the reduction of BPO, following the same mechanism, eqn (10).

The intensity of ECL varied from **1–4**. Compounds **1** and **4** displayed the highest ECL intensities with photocurrents around 100 nA for **1** and 180 nA for **4**. The efficiencies for these compounds were in a range between 0.33 to 1.48% for **1** and 0.54 to 2.33% for **4**. Compounds **2** and **3** had lower ECL intensities, relative to **1** and **4**, with photocurrents around 85 nA for **2** and 30 nA for **3**. The efficiencies were in a range between 0.73 to 0.86% for **2** and 0.24 to 0.39% for **3**.

ECL was enhanced when the applied potential was pulsed in the cathodic region between 0.000 V and the low limit potential value for the compound reduction as obtained from CV experiments with a pulse width of 0.1 s. Instead of slowly scanning the potential from 0.000 V to −2.278 V shown in Fig. 5, the working electrode was pulsed quickly between these potential values and an increase in intensity of ECL was observed. The efficiencies for these compounds were 0.71% for **1**, 0.20% for **2**, 0.25% for **3**, and 1.87% for **4**. Pulsing generates radical cations and anions in a faster alternative pace and reduces the decay of the unstable radicals, leading to greater occasions for the cations and anions to meet, react, and emit light.

3.4 ECL spectroscopy

Fig. 6 shows the coreactant ECL spectra of **1–4** with BPO during the pulsing of the applied potential in the cathodic regions (till the reduction of the compounds). The spectrum for **1** in the coreactant system was fitted to one peak centered at 515 nm, Fig. 6(a) (see spectra with curve-fitting, Fig. S1, in the ESI†). The peak at 515 nm was red-shifted relative to that in PL by 140 nm. The long wavelength ECL can be assigned to emission from excimers.³⁸ Excimers are excited states of dimers that can be observed in ECL of organic compounds.^{15,16} The formation of excimers might result from dimerization of the radical anion and cation or stacking of the monomer in the excited state with a monomer in the ground state due to the π conjugation of the modified nucleobase.⁵⁰ A possible mechanism for excimer growth in ECL for **1** is shown in eqn (11)–(13).⁵⁵ ThdC* can react with the ground state species ThdC to form an excimer as seen in eqn (11). Another possible route for excimer formation involves the radical cation and anion species to form the excimer,

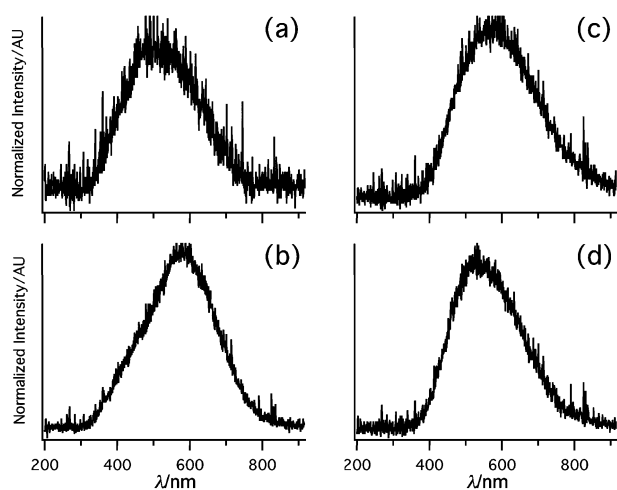
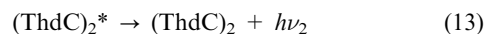
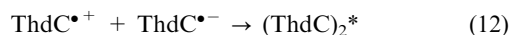


Fig. 6 ECL spectra of **1–4** in DMF containing 5.0×10^{-3} M BPO and 0.1 M TBAP as supporting electrolyte and pulsing between potential ranges from (a) 0.000 to -2.278 V, $t = 60$ s for **1**, (b) 0.000 to -2.452 V, $t = 60$ s for **2**, (c) 0.000 to -2.517 V, $t = 60$ s for **3**, and (d) 0.000 to -2.126 V, $t = 60$ s for **4**. ECL intensities were normalized by their respective peak heights.

(ThdC) $_2^*$, eqn (12). The excimer can then relax down to its ground state and emit light, eqn (13). For compound **1**, the two routes are possible:



The energy of the resulting excited species, (ThdC) $_2^*$, was lower than that of the reactants and relaxes down to the ground state, ThdC, and a longer wavelength than the monomer will be observed, similar to the spectrum of **2**, Fig. 6(b). For **2**, the spectrum showed two peaks, one at 395 nm and the second broad band at 577 nm. The peaks were red-shifted by 15 and 197 nm with respect to the PL peak seen at 380 nm. From eqn (5), (6), and (9)–(13), we observed excited monomer and excimer formation from the two given pathways. It appears that as conjugation increases in the modified nucleosides, ECL emission becomes more red-shifted. Compound **3**, Fig. 6(c), showed one maximum at 588 nm and displayed the most significant red-shift of 208 nm relative to the PL peak at 380 nm. Furthermore, the maximum wavelength of compound **4**, Fig. 6(d), was at 556 nm, red-shifted to PL by 171 nm respectively. The growth in excimer formation was more easily observed with **2**, Fig. 6(b), and the most red-shifted compounds were **2**, **3** and **4**. We can conclude that compounds **1–4** can easily form excimers, however there was a combination of monomers and excimers present in ECL system **2** by pulsing the electrode potential.

The crystal structures of **1** (this work) and **2**³⁸ illustrate the coplanar shape of the conjugated aromatic ring systems for these four compounds, allowing the π electrons to delocalize over the aromatic ring systems and therefore lowering the band gap between the HOMO and LUMO. This enhances the effective conjugation length and consequently causes emission

peak to red-shift relative to the photoluminescence (PL) peaks as previously reported.³⁸

4. Conclusions

We have determined the redox potentials and calculated the ECL efficiencies of a series of modified triazolyldeoxycytidine nucleosides, **1–4**. With increasing conjugation in the lumino-phore, we observed a decrease in the separation between first oxidation and reduction peaks of the compounds. The annihilation ECL efficiencies were weak relative to DPA, ranging from 0.40 to 0.52% for **1**, 0.39 to 0.41% for **2**, 0.71 to 1.08% for **3**, and 0.10 to 0.24% for **4**. The efficiencies increased in the coreactant systems with ECL efficiencies ranging from 0.33 to 1.48% for **1**, 0.73 to 0.86% for **2**, 0.24 to 0.39% for **3**, and 0.54 to 2.33% for **4**. The ECL spectra were red-shifted relative to the corresponding PL spectra previously reported with wavelengths ranging from 515 nm for **1**, 395 and 577 nm for **2**, 588 nm for **3**, and 556 nm for **4**. The generation of excimers in **1–4**, with the monomer still present in **2**, was observed in the ECL systems studied. The radical anions and cations generated in solution follow two pathways, *via* electron transfer, and combination of electron transfer and dimerization, forming excited species and excimers. Incorporating these modified nucleosides into ssDNA, and hybridizing the modified ssDNA with a complementary ssDNA or a single-base mis-matched ssDNA may allow for an ECL readout which could give information on the nature of the mismatch, thereby leading to an effective means of SNP typing. ECL is a fast, cost effective technique that requires low quantity and is highly selective, sensitive, and tunable with our electro-chemical instrumentation and detection systems. Using ECL detection with these modified nucleosides is in progress towards SNP typing of genes pertinent to various human genetic disorders.

Acknowledgements

We thank the Natural Sciences and Engineering Research Council (NSERC, Canada) for generous financial support through the Discover Grant and Research Tools and Instruments Grant programs. DWD acknowledges an NSERC Canada Graduate Scholarship (CGS-D). Additionally, we would like to acknowledge Dr P.J. Ragona, and Dr D. W. Shoosmith, for use of their instruments, John Vanstone and Jon Aukema (Electronics Shop), Yves Rambour (Glassblowing Shop) for their technical service, and the Department of Chemistry at The University of Western Ontario for supporting graduate research.

References

- 1 A. J. Bard, in *Electrogenerated Chemiluminescence*, ed. A. J. Bard, Marcel Dekker, Inc., New York, 2004.
- 2 D. M. Hercules, *Science*, 1964, **145**, 808–809.
- 3 R. E. Visco and E. A. Chandross, *J. Am. Chem. Soc.*, 1964, **86**, 5350–5351.
- 4 K. S. V. Santhanam and A. J. Bard, *J. Am. Chem. Soc.*, 1965, **87**, 139–140.
- 5 R. Pyati and M. M. Richter, *Annu. Rep. Prog. Chem., Sect. C*, 2007, **103**, 12–78.
- 6 M. M. Richter, *Chem. Rev.*, 2004, **104**, 3003–3036.

- 7 S. Kulmala and J. Suomi, *Anal. Chim. Acta*, 2003, **500**, 21–69.
- 8 K. A. Fährnich, M. Pravda and G. G. Guilbault, *Talanta*, 2001, **54**, 531–559.
- 9 A. W. Knight, *TrAC, Trends Anal. Chem. (Pers. Ed.)*, 1999, **18**, 47–62.
- 10 D. Laser and A. J. Bard, *J. Electrochem. Soc.*, 1975, **122**, 632–640.
- 11 W. Miao, *Chem. Rev.*, 2008, **108**, 2506–2553.
- 12 L. Hu and G. Xu, *Chem. Soc. Rev.*, 2010, **39**, 3275–3304.
- 13 S. Krishnan, E. G. Hvastkovs, B. Bajrami, D. Choudhary, J. B. Schenkman and J. F. Rusling, *Anal. Chem.*, 2008, **80**, 5279–5285.
- 14 J. F. Rusling, E. G. Hvastkovs, D. O. Hull and J. B. Schenkman, *Chem. Commun.*, 2008, 141–154.
- 15 R. Y. Lai, J. J. Fleming, B. L. Merner, R. J. Vermeij, G. J. Bodwell and A. J. Bard, *J. Phys. Chem. A*, 2004, **108**, 376–383.
- 16 J.-P. Choi, K.-T. Wong, Y.-M. Chen, J.-K. Yu, P.-T. Chou and A. J. Bard, *J. Phys. Chem. B*, 2003, **107**, 14407–14413.
- 17 T. G. Drummond, M. G. Hill and J. K. Barton, *Nat. Biotechnol.*, 2003, **21**, 1192–1199.
- 18 X. Xu and A. Bard, *J. Am. Chem. Soc.*, 1995, **117**, 2627–2631.
- 19 C. A. Marquette and L. J. Blum, *Anal. Bioanal. Chem.*, 2008, **390**, 155–168.
- 20 W. Miao and A. J. Bard, *Anal. Chem.*, 2003, **75**, 5825–5834.
- 21 K. Furukawa, H. Abe, J. Wang, M. Uda, H. Koshino, S. Tsuneda and Y. Ito, *Org. Biomol. Chem.*, 2009, **7**, 671–677.
- 22 E. Pinnisi, *Science*, 1998, **281**, 1787–1789.
- 23 S. Tyagi, D. P. Bratu and F. R. Kramer, *Nat. Biotechnol.*, 1998, **16**, 49–53.
- 24 A. P. Silverman and E. T. Kool, *Chem. Rev.*, 2006, **106**, 3775–3789.
- 25 X. Li and D. R. Liu, *Angew. Chem., Int. Ed.*, 2004, **43**, 4848–4870.
- 26 S. Tyagi and F. R. Kramer, *Nat. Biotechnol.*, 1996, **14**, 303–308.
- 27 A. Okamoto, K. Tanaka, T. Fukuta and I. Saito, *J. Am. Chem. Soc.*, 2003, **125**, 9296–9297.
- 28 A. Okamoto, K. Tanaka, T. Fukuta and I. Saito, *ChemBioChem*, 2004, **5**, 958–963.
- 29 J. Zhang, X. J. Sun, K. M. Smith, F. Visser, P. Carpenter, G. Barron, Y. S. Peng, M. J. Robins, S. A. Baldwin, J. D. Young and C. E. Cass, *Biochemistry*, 2006, **45**, 1087–1098.
- 30 L. F. Liu, Y. F. Li, D. Liotta and S. Lutz, *Nucleic Acids Res.*, 2009, **37**, 4472–4481.
- 31 J. A. Secrist, J. R. Barrio and N. J. Leonard, *Science*, 1972, **175**, 646–647.
- 32 N. K. Andersen, L. Spáčilová, M. D. Jennings, P. Kočalka, F. Jensen and P. Nielsen, Joint Symposium of the 18th International Roundtable on Nucleosides, Nucleotides and Nucleic Acids and the 35th International Symposium on Nucleic Acids Chemistry, Kyoto, Japan, 2008.
- 33 M. E. Hassan, *Nucleosides Nucleotides*, 1991, **10**, 1277–1283.
- 34 D. Peters, A.-B. Hörnfeldt, S. Gronowitz and N. G. Johansson, *Nucleosides Nucleotides*, 1992, **11**, 1151–1173.
- 35 M. Mizuta, J.-I. Banba, T. Kanamori, R. Tawarada, A. Ohkubo, M. Sekine and K. Seio, *J. Am. Chem. Soc.*, 2008, **130**, 9622–9623.
- 36 N. E. Tokel-Takvoryan, R. E. Hemingway and A. J. Bard, *J. Am. Chem. Soc.*, 1973, **95**, 6582–6589.
- 37 K. N. Swanick, D. W. Dodd, R. H. E. Hudson, Z. Ding and N. D. Jones, 19th QOMSBOC, Toronto, Canada, 2008.
- 38 D. W. Dodd, K. N. Swanick, J. T. Price, A. L. Brazeau, M. J. Ferguson, N. D. Jones and R. H. E. Hudson, *Org. Biomol. Chem.*, 2010, **8**, 663–666.
- 39 P. Kočalka, N. K. Andersen, F. Jensen and P. Nielsen, *ChemBioChem*, 2007, **8**, 2106–2116.
- 40 V. Munshi, M. Lu, P. Felock, R. J. O. Barnard, D. J. Hazuda, M. D. Millers and M.-T. Lai, *Anal. Biochem.*, 2008, **374**, 121–132.
- 41 H. C. Kolb, M. G. Finn and K. B. Sharpless, *Angew. Chem., Int. Ed.*, 2001, **40**, 2004–2021.
- 42 H. C. Kolb and K. B. Sharpless, *Drug Discovery Today*, 2003, **8**, 1128–1137.
- 43 P. Wu and V. V. Folkin, *Aldrichimica Acta*, 2007, **40**, 7–17.
- 44 P. Wu, A. K. Feldman, A. K. Nugent, C. J. Hawker, A. Scheel, B. Voit, J. Pyun, J. M. J. Fréchet, K. B. Sharpless and V. V. Folkin, *Angew. Chem., Int. Ed.*, 2004, **43**, 3928–3932.
- 45 A. J. Bard, Z. Ding and N. Myung, in *Structure & Bonding*, Springer Berlin/Heidelberg, 2005, vol. 118, pp. 1–57.
- 46 R. M. Cerviño, W. E. Triaca and A. J. Arvia, *J. Electroanal. Chem.*, 1985, **182**, 51–60.
- 47 S. K. Haram, B. M. Quinn and A. J. Bard, *J. Am. Chem. Soc.*, 2001, **123**, 8860–8861.
- 48 K. M. Omer, S.-Y. Ku, K.-T. Wong and A. J. Bard, *Angew. Chem., Int. Ed.*, 2009, **48**, 9300–9303.
- 49 R. Bezman and L. R. Faulkner, *J. Am. Chem. Soc.*, 1972, **94**, 6317–6323.
- 50 C. Booker, X. Wang, S. Haroun, J. Zhou, M. Jennings, B. L. Pagenkopf and Z. Ding, *Angew. Chem., Int. Ed.*, 2008, **47**, 7731–7735.
- 51 W. L. Wallace and A. J. Bard, *J. Phys. Chem.*, 1979, **83**, 1350–1357.
- 52 A. J. Bard and L. R. Faulkner, *Electrochemical methods, fundamentals and applications*, John Wiley & Sons Inc., New York, 2nd edn, 2001.
- 53 H. H. Girault, *Électrochimie Physique et Analytique*, Presses Polytechnique et Universitaires Romandes, Lausanne, Switzerland, 2001.
- 54 Z. Ding, B. M. Quinn, S. K. Haram, L. E. Pell, B. A. Korgel and A. J. Bard, *Science*, 2002, **296**, 1293–1297.
- 55 I. Prieto, J. Teetsov, M. A. Fox, D. A. Vanden Bout and A. J. Bard, *J. Phys. Chem. A*, 2001, **105**, 520–523.